Mechanism for Calcium Ion Sensing by the C2A Domain of Synaptotagmin I

Jacob W. Gauer,[†] Ryan Sisk,[†] Jesse R. Murphy,[†] Heathere Jacobson,[†] R. Bryan Sutton,[‡] Gregory D. Gillispie,[§] and Anne Hinderliter[†*]

[†]Department of Chemistry and Biochemistry, University of Minnesota Duluth, Duluth, Minnesota; [‡]Department of Cell Physiology, Texas Tech University Health Sciences Center, Lubbock, Texas; and [§]Fluorescence Innovations, Bozeman, Montana

ABSTRACT The C2A domain is one of two calcium ion (Ca^{2+})- and membrane-binding domains within synaptotagmin I (Syt I), the identified Ca^{2+} sensor for regulated exocytosis of neurotransmitter. We propose that the mechanistic basis for C2A's response to Ca^{2+} and cellular function stems from marginal stability and ligand-induced redistributions of protein conformers. To test this hypothesis, we used a combination of calorimetric and fluorescence techniques. We measured free energies of stability by globally fitting differential scanning calorimetry and fluorescence lifetime spectroscopy denaturation data, and found that C2A is weakly stable. Additionally, using partition functions in a fluorescence resonance energy transfer approach, we found that the Ca^{2+}- and membrane-binding sites of C2A exhibit weak cooperative linkage. Lastly, a dye-release assay revealed that the Ca^{2+}- and membrane-bound conformer subset of C2A promote membrane disruption. We discuss how these phenomena may lead to both cooperative and functional responses of Syt I.

INTRODUCTION

Neuronal proteins are suspended in a network of interacting entities. One such network leads to the regulated exocytosis of neurotransmitters. Upon release from the presynaptic cell, the neurotransmitter diffuses across the synaptic cleft and binds to receptors in the postsynaptic cell, invoking one of many possible physiological responses. The neurotransmitter is released from active-zone synaptic vesicles positioned in the vicinity of the plasma membrane. However, the combination of interactions that culminates in the release of vesicle contents is poorly understood. The synaptic vesicle is populated by 14 distinct proteins and 9 lipid species with widely different relative concentrations (1). Furthermore, the plasma membrane-associated components of the active zone are dynamic because they reside within a diffuse and shifting membrane surface that can alter the distribution of additional interacting partners. The numbers of protein and lipid species, differences in relative concentrations, and overall dynamic distribution within the synaptic vesicle active zone lead to potentially millions of possible interaction combinations, a small number of which lead to neurotransmitter release.

Within this large number of possible combinations, investigators have defined an initiating signal for neurotransmitter release: a rise in intracellular calcium ion (Ca^{2+}) and its subsequent chelation by synaptotagmin I (Syt I) (2–6). The Syt I protein comprises two Ca^{2+} chelating C2 domains, C2A and C2B, that are tethered to the vesicle membrane by a single N-terminal transmembrane helix (7). Syt I has a number of binding partners, most notably the SNARE complex, complexin, membranes enriched in acidic phospholipid, and Ca^{2+} (8–10).

The mechanism by which Syt I responds to Ca^{2+} upon chelation has not been definitively established, but it is not due to large-scale structural changes in the isolated C2 domains (11). Moreover, the biological consequences of Ca^{2+} binding by Syt I are nuanced. Syt I is not only the sensor for baseline synaptic transmission, it can also function as a redundant sensor for synaptic facilitation (i.e., the enhancement of a second postsynaptic response in a pair of closely separated presynaptic stimuli) (12). Attempts to understand Syt I's mechanism are further complicated by the fact that the functional endpoint varies with the combination of binding partners involved. Single-vesicle docking and fusion assays have revealed several heterogeneous pathways for both processes, where Syt I and Ca^{2+} accelerated docking but bilayer fusion was the rate-limiting step (13). In contrast, bulk vesicle fusion assays including SNARE proteins showed an increase in SNARE-driven vesicle docking upon addition of Syt I and Ca^{2+}, with docking rather than fusion being the rate-limiting step (14).

These diverse observations, the most pertinent of which are a lack of substantial structural changes in each of the isolated C2 domains upon binding of ligand and an inherent functional plasticity, suggest a unifying model for Syt I function: environmental responsiveness and signal dissemination that results from marginal stability. In this model, marginal stability provides a means of achiving both a cooperative response and functional fine-tuning. Binding of Ca^{2+}, for instance, specifically stabilizes distinct

Submitted December 22, 2011, and accepted for publication May 29, 2012.

*Correspondence: ahinderl@d.umn.edu

Gregory D. Gillispie's present address is Department of Biochemistry, Molecular Biology, and Biophysics, University of Minnesota, Minneapolis, MN.

Editor: William Wimley.

0006-3495/12/07/0238/9 $2.00

http://dx.doi.org/10.1016/j.bpj.2012.05.051

conformations (also known as conformers) that are cation-binding competent. Ca^{2+} binding causes the overall conformational equilibrium (collectively called the conformer ensemble) to shift and repopulate the now-depleted binding-competent conformer, allowing for additional binding and subsequent redistribution (Fig. 1). This cycle of binding and redistributing repeats and creates a feed-forward mechanism that eventually depletes all nonbinding-competent conformers, resulting in a cooperative response. If Syt I had only two conformational states (for instance, one that initiates SNARE complex assembly and one that does not), only two functional outcomes would result. Although this would be efficient, such a model implies a robust free energy of stability, which would limit interconversion between conformers and result in a nonmodifiable response that would be inconsistent with the diverse in vitro and in vivo observations of Syt I function. If instead Syt I is marginally stable and has numerous conformational states, with small subsets of conformers possessing unique physiological ramifications, more intermediate and diverse functional outcomes would be possible.

To test this multifaceted hypothesis, we applied a combination of calorimetric and spectroscopic methods to the human Syt I C2A domain. We measured the free energy of stability by fitting differential scanning calorimetry (DSC) and fluorescence lifetime spectroscopy (FLT) thermal denaturations to a two-state model of protein unfolding. We assessed the binding properties of the domain using fluorescent cation and lipid probes in fluorescence resonance energy transfer (FRET). We then assessed membrane disruption, a distinct functionality of Syt I that enhances membrane fusion (15–18), using a carboxyfluorescein-containing liposome efflux assay.

In this study, we found that C2A has an anomalously low free energy of stability. This stability, which we suggest correlates to its distribution of conformers, is distinct for the combinations of ligands examined. Furthermore, the Ca^{2+}- and membrane-bound conformations of C2A, in which we find a weak cooperative linkage between ligand-binding sites, contributes to membrane disruption of liposomes enriched in phosphatidylserine. These findings are consistent with the hypothesis that C2A undergoes ligand-specific conformer redistributions resulting in the differential selection of conformer subsets that facilitate specific functional outcomes.

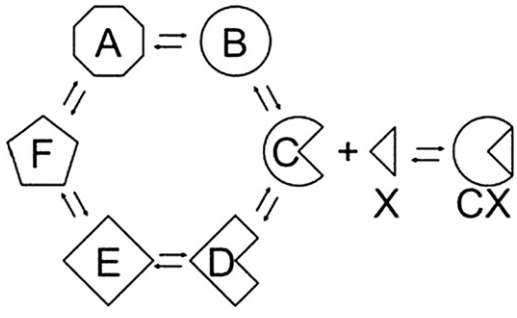

FIGURE 1 Linked conformational and binding equilibria: a schematic of a simplified version of the general model. A–F represents different conformers; X represents ligand.

MATERIALS AND METHODS

Materials

1-Palmitoyl-2-oleoyl-*sn*-glycero-3-phosphocholine (POPC or 16:0,18:1PC), 1-stearoyl-2-oleoyl-*sn*-glycero-3-phosphocholine (SOPC or 18:0,18:1PC), 1-palmitoyl-2-oleoyl-*sn*-glycero-3-phospho-L-serine (POPS or 16:0,18:1PS), 1-stearoyl-2-oleoyl-*sn*-glycero-3-phospho-L-serine (SOPS or 18:0,18:1PS), and Dansyl di16:0-phosphatidylethanolamine (DHPE) were obtained from Avanti Polar Lipids (Birmingham, AL). Potassium chloride (KCl) was puriss-grade, and 3-(*N*-morpholino)propanesulfonic acid (MOPS) and calcium chloride dihydrate were BioChemika grade (Fluka Chemical). Terbium (III) chloride hexahydrate was obtained from Invitrogen Molecular Probes (Eugene, OR). All buffers used were decalcified with the use of Chelex-100 ion-exchange resin (Bio-Rad Labs).

Preparation of large unilamellar vesicles

We prepared large unilamellar vesicles (LUVs) by aliquoting stock solutions of lipid in chloroform into borosilicate culture tubes using gas-tight syringes (Hamilton, Reno, NV). Samples were dried to a thin film under a gentle stream of argon and dried briefly under a vacuum of <20 mTorr before being lyophilized from benzene/methanol (19/1, v/v). Lipids were hydrated with decalcified 20 mM MOPS, 100 mM KCl, pH 7.5, in the dark above their gel-fluid phase transition temperature under argon. LUVs were prepared by extruding a multilamellar vesicle dispersion through a sandwich of prefilters around a 0.1 μm pore size polycarbonate filter (Avanti Polar Lipids) at least 31 times (19). All lipid concentrations were determined by means of the phosphate assay described by Kingsley and Feigenson (20).

Purification of human Syt I C2A domain

Human Syt I C2A was purified as a glutathione S-transferase (GST) fusion protein via affinity chromatography, followed by removal of the GST domain. Final purity was determined to be >95% by SDS-PAGE densitometry. Final concentrations were determined using a Nanodrop with an A280 extinction coefficient of 12,090 $cm^{-1}M^{-1}$. For more extensive details, refer to the Supporting Material.

DSC

DSC experiments were performed on a NanoDSC (TA Instruments, New Castle, DE) using protein concentrations of ~0.2 mg/ml and a scan rate of 1°C/min. These scans were conducted in 20 mM MOPS, 100 mM KCl, pH 7.5, which was chelexed to remove any trace Ca^{2+}. For scans that were performed in the absence of calcium ion, the samples contained 500 μM EGTA to further ensure Ca^{2+}-free conditions. Scans conducted in the presence of Ca^{2+} used concentrations such that the protein's Ca^{2+}-binding sites were 95% saturated. Scans performed in the presence of lipid membranes were designed to contain an excess of negatively charged phospholipids. The phospholipids were LUVs composed of a 60:40 mixture of 16:0,18:1PC and 16:0,18:1PS. The denaturation profiles were carried out with 40% PS to ensure that the protein would be fully bound to the membrane when the membrane-associated states were characterized. By comparing the measured enthalpies from two scans of the same sample

(for all replicates under each set of conditions), we determined a range of 60–90% reversibility. Displaying reversibility was important not only because it allows for the data to be analyzed using reversible thermodynamics but also because normal biological processes are generally not irreversible.

FLT

FLT experiments were performed on a Lifetime spectrometer (Fluorescence Innovations, Bozeman, MT) using protein concentrations of 0.03 mg/ml. These scans were conducted in chelexed 20 mM MOPS, 100 mM KCl, pH 7.5. The lifetime spectrometer is specifically tuned to excite C2A's single endogenous tryptophan at 295 nm, allowing for uniquely sensitive detection of changes in fluorescence signal. The intrinsic fluorescence of this tryptophan was monitored as a function of increasing temperature in 2°C increments. An emission spectrum consisting of just the integrated intensity of the lifetime decay (no time-resolved or lifetime measurements were made in this study) was collected from 310 nm to 360 nm, and data collected at 340 nm were used in the analysis. The 340 nm wavelength had the strongest contribution from tryptophan, with little contribution from water fluorescence. Changes in the fluorescence emission (hereafter referred to as integrated fluorescence intensity) at other wavelengths were separately analyzed to confirm that the data collected at 340 nm were representative of the signal change associated with the unfolding transition. When applicable, a background of 500 μM EGTA was used to ensure Ca^{2+}-free conditions. In scans containing Ca^{2+}, concentrations corresponded to 95% saturation. Scans in the presence of lipid membranes were designed to contain an excess of negatively charged phospholipids. The phospholipid vesicles were identical in composition to that described above for the DSC samples. The denaturation profiles were carried out with 40% PS to ensure that the protein would be fully bound to the membrane when the membrane-associated states were characterized. By comparing the integrated fluorescence intensity of the sample before heating and after cooling, we determined a percent reversibility of 80–90% for lipid-free conditions, and 60–70% when lipid was present.

Fluorescence spectroscopy binding assay

We determined the binding affinity of Syt I C2A for Tb^{3+} and lipid by interpreting the FRET from the single tryptophan in C2A to bound Tb^{3+}. The lanthanide Tb^{3+} is a mimic for Ca^{2+} because it has a similar ionic radius but higher charge density. We generated cation-binding curves by monitoring the quenching of fluorescence from the single tryptophan residue in Syt I C2A. The excitation and emission wavelengths used were 295 nm and 343 nm, respectively. The loss of signal was normalized as fractional saturation, and ligand concentrations were corrected to account for free and bound ligand using the binding stoichiometry. Finally, the bound ligand was subtracted from the total ligand added at each point, resulting in free ligand. All binding curves were then plotted as fractional saturation versus free ligand concentration.

To measure the lipid-binding affinity of C2A directly, we titrated a membrane doped with the fluorescent probe Dansyl DHPE into a C2A suspension. Data were collected in a manner similar to that employed for the Tb^{3+} titrations. The data were plotted as fractional saturation versus free lipid concentration, assuming that C2A binds five lipids. The term "free lipid concentration" refers to free exterior lipid concentration, which is assumed to be half of the total lipid concentration because the protein only has access to the outer leaflet of the LUV.

All titrations were done using a Fluorolog steady-state fluorimeter (Horiba Jobin Yvon) with double emission and double excitation monochromators interfaced to a Neslab water bath and thermostated at 20°C with 0.4–0.5 μM C2A in decalcified 2 mM MOPS, 100 mM KCl, pH 7.5 buffer. All samples were prepared in a quartz cuvette with the use of gas-tight Hamilton syringes. After each ligand addition, the sample was gently vortexed and allowed to equilibrate for 10 min before scanning. To quantify the contribution of photobleaching to decreases in fluorescence intensity, we conducted time-trace experiments for each experimental condition and found that it contributed a negligible signal loss.

Carboxyfluorescein release assay

The fluorescence signal of LUVs containing carboxyfluorescein buffer (20 mM MOPS, 100 mM KCl, 0.02% NaN_3, and 50 mM 5-(and-6)-carboxyfluorescein (Invitrogen), pH 7.5) was measured using excitation and emission wavelengths of 492 nm and 519 nm, respectively. For these experiments, the mixture of 16:0,18:1PC and 16:0,18:1PS lipids used in both denaturation and binding studies were replaced with 18:0,18:1PC and 18:0,18:1PS lipids to increase the transition temperature to widen the experimental window with regard to changes in temperature. (For additional details, refer to the Supporting Material.) Lipid samples were brought to a total lipid concentration of 120 μM and total volume of 500 μL using an equiosmolar column equilibration buffer (20 mM MOPS, 100 mM KCl, 0.02% NaN_3, pH 7.5) before scanning. When applicable, the samples contained 117 μM Ca^{2+}; samples containing Syt I C2A had a total protein concentration of 1.60 μM. These conditions represent >95% saturation of the protein's cation-binding sites. The experiments were run for 30 min as the temperature was brought from 20°C to 0°C by means of a temperature-controlled jacket. We confirmed that the liposomes contained carboxyfluorescein by monitoring fluorescence changes upon addition of Triton X-100 detergent. All fluorescence measurements were performed on a Fluorolog 3 spectrophotometer (Horiba Jobin Yvon) in a quartz cuvette.

Analysis

DSC and FLT global fitting

We determined the free energy associated with the stability of the protein structure by globally fitting the denaturation data obtained with two techniques to a two-state transition model. In this model, a conformationally flexible protein is assumed to exist in either a native (N) or a denatured (D) ensemble, wherein conformers of each ensemble have similar energies. The transition between native and denatured ensembles occurs with no unfolding intermediates. In this way, the unfolding transition can be described by the equilibrium constant $K = [D]/[N]$.

In the DSC experiments, the heat capacity as a function of temperature $C_p(T)$ can be described in terms of the overall enthalpy of the transition ($\Delta H(T)$) and the fraction of the protein that has gone through the transition (f_D):

$$C_p(T) = \frac{d}{dT}(\Delta H(T) f_D). \quad (1)$$

Both $\Delta H(T)$ and f_D can be expressed in terms of the reference-state thermodynamic parameters, specifically the enthalpy of the transition (ΔH_{Tm}), the transition temperature (T_m), and the change in the baseline heat capacity (ΔC_p):

$$C_p(T) = \frac{d}{dT}\left(\frac{K(\Delta H_{Tm} + \Delta C_p(T - T_m))}{(1 + K)}\right), \quad (2)$$

where $K = \exp[\Delta H_{Tm}/R\,(1/T_m - 1/T) + \Delta C_p/R\,(T_m/T - 1 + \ln(T/T_m))]$, and R is the ideal gas constant. By comparing the fit parameter enthalpy above with the actual calorimetric enthalpy (ΔH) in a $\Delta H_{Tm}/\Delta H$ ratio, we were able to assess the validity of the two-state assumption.

In the FLT experiments, the integrated fluorescence intensity of Syt I C2A's single endogenous tryptophan was measured. The single tryptophan's fluorescence is highly sensitive to changes in its local chemical environment. The observed fluorescent signal, S(T), is a composite of signals coming from both native (S_N) and denatured (S_D) states weighted by the

fraction of the protein existing in each state. The composite signal can be related to the equilibrium constant as follows:

$$S(T) = S_D + \frac{(S_N - S_D)}{(1 + K)}, \quad (3)$$

where signals associated with the native and denatured states are assumed to be linear and thus described as $S_N = m_N T + b_N$ and $S_D = m_D T + b_D$ (21). As before, with simple substitutions, Eq. 3 can be expressed in terms of the reference-state thermodynamic parameters, ΔH_{Tm}, T_m, and ΔC_p. The composite signal measured (S(T) in Eq. 3) was normalized to the calculated intensities from the two-state model and subsequently displayed as Intensity in the corresponding plots.

We fit these data simultaneously by nonlinear least-squares regression analysis using ΔH_{Tm}, T_m, and ΔC_p as global fitting parameters (22). Four replicates of each technique (for a total $N = 8$) were used for each ligand condition (ligand-free, in the presence of saturating Ca^{2+}, in the presence of excess phospholipid, and in the presence of both Ca^{2+} and phospholipid). Each data point within each technique is the average of the four replicates, with the associated error plotted as a 95% confidence interval. The model line is the global fit of eight data sets, and we determined the associated error with the fit using an approach described by De Levie (23).

We observed that of these parameters, ΔC_p was the most loosely constrained by the fit, especially in the presence of Ca^{2+}. This loose constraint was likely due to variation in the DSC baseline associated with denatured protein. Also, this parameter did not have a significant impact on the overall shape of the calculated FLT fit line. Therefore, the FLT data sets provided little or no additional constraint on the parameter. Fortunately, in the absence of all ligands, the ΔC_p fit parameter was in good agreement with a theoretical value (24). Thus, to constrain the fits in the presence of ligand, ΔC_p was assumed to be a constant 1.92 kcal/mole across all ligand conditions.

After obtaining the global fit parameters (ΔH_{Tm}, T_m, and ΔC_p), we calculated the free energy of stability at the physiological temperature of 37°C ($\Delta G^\circ_{37^\circ C}$) using the Gibbs-Helmholtz equation:

$$\Delta G^\circ = \Delta H_{Tm}\left(1 - \frac{T}{T_m}\right) + \Delta C_p\left[T - T_m - T\left(\ln\left(\frac{T}{T_m}\right)\right)\right]. \quad (4)$$

The above calculation was performed for all ligation states of the C2A domain. Lastly, we calculated the change in entropy for the unfolding reaction (ΔS) using $\Delta G^\circ_{37^\circ C}$, the physiological temperature of 310 K, and ΔH_{Tm} in the Gibbs free-energy equation

$$\Delta G^\circ = \Delta H - T\Delta S. \quad (5)$$

Binding isotherms and partition functions

Binding partition functions were derived as described previously (25) from the thermodynamic cycle (Fig. S1 in Supporting Material) such that they contained a term proportional to the probability of observing each state of the protein. The binding isotherm (θ) can be calculated from the partition function (Q), by the following derivative:

$$\theta = \frac{[X]}{NQ}\frac{dQ}{d[X]}, \quad (6)$$

where θ is the fractional saturation of cation-binding sites on C2A, or the fraction of protein bound to lipid; X refers to free ligand (i.e., unbound) [Tb^{3+}], [Ca^{2+}], or [Lipid]; N is the number of ligand-binding sites (when X refers to [Tb^{3+}] or [Ca^{2+}], $N = 2$ in the absence of lipid, and $N = 3$ in the presence of lipid (26), and when X refers to [L], $N = 1$ because the protein binds to a single liposome), and Q is the partition function. In solution, the cation binding of C2A can be described by the partition function q_0:

$$q_0 = 1 + 2K_a[X] + K_a^2[X]^2, \quad (7)$$

where K_a is the cation association constant.

A third cation-binding site in Syt I C2A becomes more probable in the presence of acidic phospholipid-containing membranes because it binds with affinity σK_a (27). The cooperative factor σ is the enhancement of binding of the third cation. This transition can be modeled by the global partition function below:

$$Q = q_0 + K_L[L]q_1, \quad (8)$$

where K_L is the lipid-binding constant and q_1 is described by

$$q_1 = 1 + 2K_a[X] + K_a^2[X]^2 + \sigma K_a^3[X]^3. \quad (9)$$

One can calculate the binding isotherm (θ), which is used to fit the binding plots, for cation and lipid binding by differentiating between the partition functions with respect to either ligand ([X] or [L]). In the case of lipid binding in the absence of cation, the partition function is as follows:

$$Q_L = 1 + K_L[L]. \quad (10)$$

RESULTS

Determination of the free energy of stability for C2A

To stringently determine the free energies of stability in the presence and absence of Ca^{2+} and lipid ligands, we thermally denatured C2A using both DSC and FLT methods. The resulting data sets were then globally fit to a two-state model of protein unfolding. Fig. 2 shows the average of four calorimetric (*A–D*) and spectroscopic (*E–H*) denaturation experiments under all ligation conditions. There was notable variation between replicate measurements, especially in the presence of both Ca^{2+} and membranes. Table 1 shows the thermodynamic parameters resulting from the global fit and includes the calculated free energy of stability at physiological temperature ($\Delta G^\circ_{37^\circ C}$). Note that relative to proteins of a similar size, these free-energy values are low (28,29).

Binding assays

To quantify ligand binding and the degree of cation- and membrane-binding-site linkage, we measured the binding profiles using Tb^{3+} and DHPE FRET probes, and fit them using a global partition function approach (26,30,31). An independent site model (Fig. 3 *A*, *solid circles*) described C2A as binding two terbium cations with equal affinity ($K_a = 5 \times 10^4\ M^{-1}$, $\Delta G^\circ = -6.3$ kcal/mol at 20°C). The calculated K_L of C2A toward 50:40:10 16:0,18:1PC:16:0, 18:1PS:Dansyl DHPE liposomes (Fig. 3 *B*, *solid squares*) was $3.3 \times 10^5\ M^{-1}$ ($\Delta G^\circ = -7.4$ kcal/mol at 20°C).

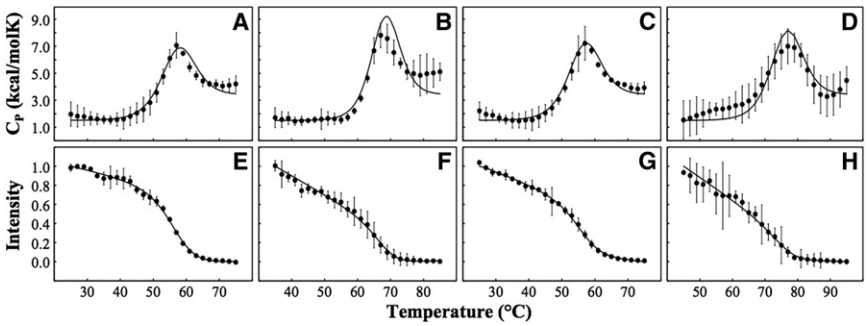

FIGURE 2 Denaturation of Syt I C2A. Data points represent the average of four trials, and error bars show 95% confidence intervals. Fit lines represent the calculated fits from the global analysis of both DSC and FLT experiments using the same set of parameters. DSC experiments were run with 13 μM Syt I C2A in the following conditions: (*A*) 500 μM EGTA, (*B*) 800 μM Ca^{2+} (representing 95% saturation), (*C*) 870 μM total phospholipid (LUVs of (60:40) 16:0,18:1PC:16:0,18:1PS) and 500 μM EGTA, and (*D*) 800 μM Ca^{2+} (representing 95% saturation) and 870 μM total phospholipid (LUVs of (60:40) 16:0,18:1PC:16:0,18:1PS). FLT experiments were run with 0.75 μM Syt I C2A in the following conditions: (*E*) 500 μM EGTA, (*F*) 770 μM Ca^{2+} (representing 95% saturation), (*G*) 50 μM total phospholipid (LUVs of (60:40) 16:0,18:1PC:16:0,18:1PS) and 500 μM EGTA, and (*H*) 770 μM Ca^{2+} (representing 95% saturation) and 50 μM total phospholipid (LUVs of (60:40) 16:0,18:1PC:16:0,18:1PS).

To test for cation- and membrane-binding-site linkage, DHPE-containing liposomes were titrated into C2A in the presence of subsaturating concentrations of Ca^{2+} (Fig. 3 *B*, *solid circles*). The slight change in K_L (2.7×10^5 M^{-1}, $\Delta G^\circ = -7.3$ kcal/mol at 20°C) suggests weak linkage under subsaturating Ca^{2+} conditions. By globally fitting the data with a fixed experimental K_L, we determined a Ca^{2+}-binding constant of 2.00×10^4 M^{-1} ($\Delta G^\circ = -5.8$ kcal/mol at 20°C, 0.5 kcal/mol less than Tb^{3+} and attributed to higher charge density of the fluorescent mimic). This Ca^{2+}-binding constant was compared against the cation constant derived from the reverse titration (Ca^{2+} titrated into C2A and DHPE liposomes) and was found to be in agreement (Fig. 3 *C*). To verify weak linkage between binding sites, Tb^{3+} was titrated into a suspension of C2A and an excess of 60:40 16:0,18:1PC:16:0,18:1PS liposomes (Fig. 3 *A*, *open circles*). The presence of membrane increased cation binding with a best fit cooperativity factor of $\sigma = 12$, consistent with induction of a third cation site (Supporting Material) having an affinity of $K_a = 6 \times 10^5$ M^{-1} ($\Delta G^\circ = -7.7$ kcal/mol at 20°C).

Carboxyfluorescein release

Syt I has been defined as a calcium sensor and is known to enhance the likelihood of membrane fusion (15–18). To test the hypothesis that within C2A's conformer ensemble a small subpopulation is functionally distinct with regard to the controlled breach of the lipid bilayer, a carboxyfluorescein efflux assay was developed. Dye efflux from vesicles cooled through their fluid-to-gel state transition temperatures was found to be ~11% (Fig. 4). In the presence of Ca^{2+}, this release was hardly affected (by no more than 1%) when compared with the reference state of lipid alone. Addition of Syt I C2A (without Ca^{2+}) also had relatively little impact on dye release, with an observed increase of only 3%. These slight changes suggest that the interactions on the vesicle surface are limited and nondisruptive. In the presence of both Syt I C2A and Ca^{2+}, however, the release of carboxyfluorescein was dramatically increased to 29%, suggesting that the cation-protein complex has much more membrane-disrupting ability.

DISCUSSION

Our purpose in this study was to test the hypothesis that the C2A domain of human Syt I samples many conformations, and only a subset of these conformers have physiological ramifications, such as membrane disruption. In the absence of Ca^{2+}, the probability of existing in these functional states is low, but not zero. In the presence of Ca^{2+}, the likelihood of existing in different functional states shifts, allowing for selectively stabilized conformers to contribute to a specific cellular function. This type of linkage between ligand binding and conformational redistributions within the C2A domain relies on marginal stability and may provide mechanistic insight into how Syt I functions as a Ca^{2+} sensor (Fig. 1).

When the C2A domain's free energy of stability was measured, it was found to be anomalously low for a protein of its size (Fig. 2) (28,29). Despite being weakly stable, the C2A domain is not intrinsically disordered. Its denaturation complies with a two-state transition, as evidenced by the

TABLE 1 Thermodynamic parameters describing synaptotagmin I C2A denaturation

	ΔH_{Tm} (kcal/mole)	ΔS (kcal/moleK)	T_m (°C)	$\Delta G^\circ_{37°C}$ (kcal/mole)	$\Delta H_{Tm}/\Delta H$
Ligand-free	58.7 ± 0.3	0.18 ± 0.01	56.0 ± 0.1	2.32 ± 0.05	0.98
Ca^{2+}	77.4 ± 0.6	0.23 ± 0.01	67.6 ± 0.1	4.23 ± 0.05	1.08
PS	61.3 ± 1.1	0.19 ± 0.02	55.5 ± 0.2	2.44 ± 0.05	1.03
Ca^{2+} and PS	72.4 ± 0.9	0.21 ± 0.01	75.6 ± 0.3	3.73 ± 0.05	0.86

PS indicates the use of LUVs consisting of a 60:40 mixture of 16:0,18:1PC and 16:0,18:1PS.

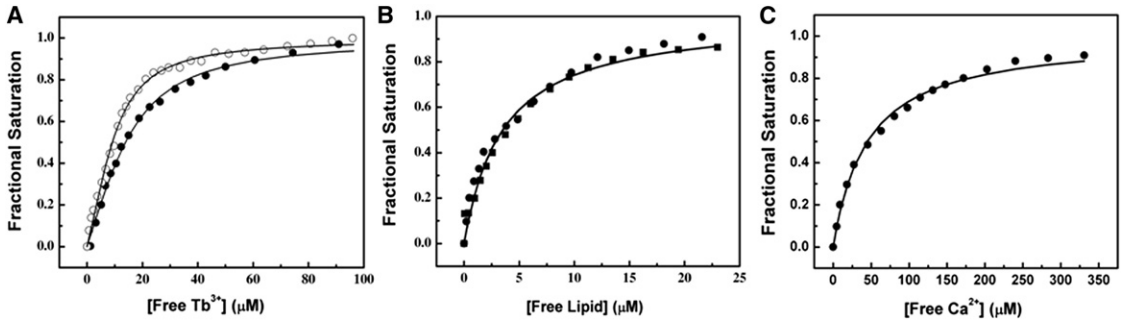

FIGURE 3 (*A*) Tb^{3+} binding to 0.4 μM Syt I C2A in the absence of lipid (*solid circles*). Tb^{3+} binding to 0.4 μM Syt I C2A in the presence of 112 μM (60:40) 16:0,18:1PC:16:0,18:1PS (*open circles*). (*B*) Titration of 0.4 μM Syt I C2A with (50:40:10) 16:0,18:1PC:16:0,18:1PS:Dansyl DHPE in the absence (*solid squares*) or presence of 2 μM Ca^{2+} (*solid circles*). (*C*) Titration of 0.4 μM Syt I C2A with Ca^{2+} in the presence of 50 μM (50:40:10) 16:0,18:1PC:16:0,18.1PS:Dansyl DHPE (*solid circles*). All titrations were carried out in decalcified 2 mM MOPS, 100 mM KCl, pH 7.5.

close agreement of directly measured and fitted enthalpies, shown as a ratio in Table 1 (32–35). Because the free energy of stability is low, however, the two-state transition is more appropriately described as a transition between two distributions of energetically similar conformers. When bound to Ca^{2+}, C2A's free energy of stability is dramatically increased and interconversion between conformations is reduced (indicated by the increase in free energy from 2.32 kcal/mole to 4.23 kcal/mole shown in Table 1). This change in free energy is notably different from membrane binding, which has a much smaller affect. This difference in the ligand-induced free-energy change could be attributed to differences between the two ligands. Ca^{2+} binding requires specific interactions between the protein and the coordination sphere of the cation. In contrast, membrane binding is much less specific. Lipids within a membrane constantly redistribute to minimize organizational free energy. Because of this organizational property, a protein would need to retain some flexibility (and therefore a low overall free energy) to interact with the dynamic membrane surface. When considering the denaturation data in their entirety, it is important to note the use of two distinct techniques. By globally fitting data from DSC (which provides a global perspective) and FLT (a more local perspective), we attempted to overcome the bias inherent to the use of either technique in isolation. When we compared the global fit with the data obtained using each technique, we observed a minor deviation between the fit and separate data sets. This observation suggests that, indeed, neither technique fully captures the unfolding process on its own. Thus, when DSC and FLT data are combined in a global fit, both the unfolding transition and measured free energies of stability better represent the C2A domain.

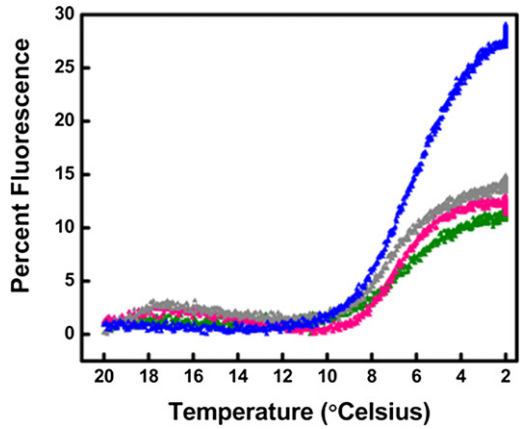

FIGURE 4 Percent fluorescence signal change of encapsulated CF leaking from 0.2 μm (80:20) 18:0,18:1PC:18:0,18:1PS lipid vesicles upon cooling. All samples contained 120 μM lipid. Green: lipid alone; magenta: 117 μM Ca^{2+} and lipid; gray: 1.60 μM Syt I C2A and lipid; blue: 1.60 μM Syt I C2A, 117 μM Ca^{2+}, and lipid.

Having established the foundation of marginal stability, we subsequently investigated binding cooperativity through the use of FRET and partition functions. The weak linkage between the Ca^{2+}- and membrane-binding sites (as shown by both the binding profiles of Fig. 3 and the cooperativity factor of $\sigma = 12$) provides a means of achieving a cooperative binding response. Because $\sigma > 1$, C2A has an increased Ca^{2+}-binding affinity (26,27). These FRET findings, when considered in the context of C2A's free energy of stability profile, may provide unique insight into Syt I's Ca^{2+}-sensing function. When C2A is bound to both Ca^{2+} and membrane, it has a lower energetic barrier between conformers compared with Ca^{2+}-bound C2A. This lower energetic barrier and increased Ca^{2+}-binding affinity implies that cooperativity stems in part from the instability of C2A resulting from its interaction with an additional dynamic ligand. When extrapolated to a broader context in which Syt I interacts with SNAREs and the inner leaflet of the plasma membrane, these findings suggest that a greater ligation state may correlate with a greater cooperative response and sensitivity to Ca^{2+}, but without loss of pliability.

The relationship between stability and function of C2A was further investigated through the use of carboxyfluorescein efflux assays. In addition to C2A's cooperative Ca^{2+}

binding, the Ca^{2+}-bound conformers were also found to enhance transient disruption of the membrane (Fig. 4). Membrane disruption was induced by decreasing the sample temperature through the liposome's fluid-to-gel phase transition. The temperature change caused not only a decrease in the number of fluid-phase acyl chain rotamers but also poor packing in more rigid, gel-state acyl chains. The packing mismatch between phases correlates with dye release and approximates the lipid mixture's transition temperature, the latter of which depends on the melting properties of the individual lipids. The hydrogen-bond capability of the phosphatidylserine headgroup is thought to account for both its higher melting temperature compared with phosphatidylcholine (36,37) and its tendency to self-aggregate among phosphatidylcholine lipids (38). The self-aggregating tendency of phosphatidylserine is accentuated by interaction with the C2A domain (39,40). It is important to note these lipid properties because under the experimental conditions tested here, there was no carboxyfluorescein release due simply to C2A binding membrane. This indicates that dye release is not due to protein-induced lipid redistribution or domain formation. Rather, the dramatic increase in dye efflux (and hence the fluorescence signal) in the presence of the Ca^{2+}-bound C2A depends on alternative factors, possibly including local curvature effects (Fig. 4).

Insight into how Ca^{2+}-bound C2A can enhance efflux comes from electron paramagnetic resonance (EPR) studies of the Syt I C2 domains. The EPR signal difference between freely-tumbling-in-solution and membrane-bound C2 domains allows for membrane-associated surfaces to be mapped (41,42). When Syt I is saturated with lipid and Ca^{2+}, the orientation of C2A and C2B within the membrane (i.e., in the midst of the lipid acyl chains) is striking. This orientation is energetically unfavorable because inclusion of the protein restricts the rotational freedom of lipid acyl chains (43,44). This orientation within the bilayer suggests that Ca^{2+}-bound C2A contributes to membrane disruption (15,16,45) and consequently promotes membrane fusion (18). Considering C2A's ability to enhance disruption in a broader context involving additional binding partners, it is possible that surrounding neuronal proteins are able to influence membrane destabilization. Although the Ca^{2+}-bound Syt I C2A is partially penetrated within the membrane, a series of lysine residues that are believed to offer a possible tether site for SNARE proteins (7) are positioned above the bilayer surface (42,46). This orientation, coupled with our findings regarding efflux, suggests that Ca^{2+}-bound C2A may link SNARE binding and membrane destabilization.

A reasonable concern regarding this study is the physiological relevance of the Ca^{2+} concentrations used in the denaturation experiments. These concentrations (~800 μM) were chosen to achieve >95% saturation of the Ca^{2+}-binding sites. Saturation ensures that the measured free energies represent a conformationally distinct distribution of states. This selective stabilization, driven by Le Chatelier's principle, is necessary to characterize the fully Ca^{2+}-bound distribution thermodynamically without any contribution from the Ca^{2+}-free distribution. In the physiological context, however, it has been observed that intracellular Ca^{2+} levels reach local concentrations of only ~20 μM in response to an action potential in the presynaptic neuron (47). This concentration corresponds to ~35% saturation with Ca^{2+}, as calculated with the cation-binding constant determined by the FRET assays. It seems, then, that the Ca^{2+} sites of Syt I C2A would not likely approach full saturation in vivo. However, this does not detract from the findings presented here. Our binding studies suggest that this low operational Ca^{2+} saturation simply promotes C2A sensitivity. An examination of the changes in C2A's fractional saturation shown in Fig. 3 *C* reveals a larger relative change at lower ranges of cation. An examination of the fractional saturation in Fig. 3 *A*, where lipid is present, shows an even greater relative change at lower ranges of cation. In both instances, the corresponding change in the probability of functionally relevant conformers should be as great at lower concentration ranges, and suggests that the system is set up for finely tuned responses.

CONCLUSION

Within a physiological context, the data presented here have implications for how Syt I functions as a calcium ion sensor and regulator of neuronal exocytosis. The low overall stability of the C2A domain suggests not only that Syt I samples many conformations but also that marginal stability underlies the cooperative binding of and sensitivity to Ca^{2+}. Despite having marginal stability, the Ca^{2+}-bound subset of conformers seems to retain enough structure to make a mechanical contribution to membrane destabilization, as evidenced by the efflux assays. These findings, coupled with Syt I's diverse functionality and large number of binding partners, suggest that other ligand- or binding-partner-induced redistributions may select for different subsets of conformers that carry out different biological functions. It is in this redistribution of conformers, which relies on marginal stability, that Syt I may function as both a calcium ion sensor and mediator of neuronal plasticity.

SUPPORTING MATERIAL

Details pertaining to protein purification, carboxyfluorescein-containing lipid vesicle preparation, and the thermodynamic cycle are available at http://www.biophysj.org/biophysj/supplemental/S0006-3495(12)00676-5.

The authors thank Samantha R. Jaworski and Michael E. Fealey for their detailed review of the manuscript and numerous suggested changes.

A.H. acknowledges support from a National Science Foundation CAREER Award (MCB-0845676). This work received partial support from the

Montana Board of Research and Commercialization Technology (grant 10-75 to G.D.G.).

REFERENCES

1. Takamori, S., M. Holt, …, R. Jahn. 2006. Molecular anatomy of a trafficking organelle. *Cell.* 127:831–846.
2. Perin, M. S., V. A. Fried, …, T. C. Südhof. 1990. Phospholipid binding by a synaptic vesicle protein homologous to the regulatory region of protein kinase C. *Nature.* 345:260–263.
3. Geppert, M., Y. Goda, …, T. C. Südhof. 1994. Synaptotagmin I: a major Ca^{2+} sensor for transmitter release at a central synapse. *Cell.* 79: 717–727.
4. Fernández-Chacón, R., A. Königstorfer, …, T. C. Südhof. 2001. Synaptotagmin I functions as a calcium regulator of release probability. *Nature.* 410:41–49.
5. Tang, J., A. Maximov, …, T. C. Südhof. 2006. A complexin/synaptotagmin 1 switch controls fast synaptic vesicle exocytosis. *Cell.* 126:1175–1187.
6. Paddock, B. E., A. R. Striegel, …, N. E. Reist. 2008. Ca^{2+}-dependent, phospholipid-binding residues of synaptotagmin are critical for excitation-secretion coupling in vivo. *J. Neurosci.* 28:7458–7466.
7. Sutton, R. B., B. A. Davletov, …, S. R. Sprang. 1995. Structure of the first C2 domain of synaptotagmin I: a novel Ca^{2+}/phospholipid-binding fold. *Cell.* 80:929–938.
8. Südhof, T. C. 2004. The synaptic vesicle cycle. *Annu. Rev. Neurosci.* 27:509–547.
9. Chapman, E. R. 2008. How does synaptotagmin trigger neurotransmitter release? *Annu. Rev. Biochem.* 77:615–641.
10. Pang, Z. P., and T. C. Südhof. 2010. Cell biology of Ca^{2+}-triggered exocytosis. *Curr. Opin. Cell Biol.* 22:496–505.
11. Shao, X., I. Fernandez, …, J. Rizo. 1998. Solution structures of the Ca^{2+}-free and Ca^{2+}-bound C2A domain of synaptotagmin I: does Ca^{2+} induce a conformational change? *Biochemistry.* 37:16106–16115.
12. Saraswati, S., B. Adolfsen, and J. T. Littleton. 2007. Characterization of the role of the synaptotagmin family as calcium sensors in facilitation and asynchronous neurotransmitter release. *Proc. Natl. Acad. Sci. USA.* 104:14122–14127.
13. Christensen, S. M., M. W. Mortensen, and D. G. Stamou. 2011. Single vesicle assaying of SNARE-synaptotagmin-driven fusion reveals fast and slow modes of both docking and fusion and intrasample heterogeneity. *Biophys. J.* 100:957–967.
14. Smith, E. A., and J. C. Weisshaar. 2011. Docking, not fusion, as the rate-limiting step in a SNARE-driven vesicle fusion assay. *Biophys. J.* 100:2141–2150.
15. Lynch, K. L., R. R. L. Gerona, …, T. F. Martin. 2008. Synaptotagmin-1 utilizes membrane bending and SNARE binding to drive fusion pore expansion. *Mol. Biol. Cell.* 19:5093–5103.
16. Martens, S., and H. T. McMahon. 2008. Mechanisms of membrane fusion: disparate players and common principles. *Nat. Rev. Mol. Cell Biol.* 9:543–556.
17. McMahon, H. T., M. M. Kozlov, and S. Martens. 2010. Membrane curvature in synaptic vesicle fusion and beyond. *Cell.* 140:601–605.
18. Kyoung, M., A. Srivastava, …, A. T. Brunger. 2011. In vitro system capable of differentiating fast Ca^{2+}-triggered content mixing from lipid exchange for mechanistic studies of neurotransmitter release. *Proc. Natl. Acad. Sci. USA.* 108:E304–E313.
19. Pokorny, A., and P. F. F. Almeida. 2004. Kinetics of dye efflux and lipid flip-flop induced by delta-lysin in phosphatidylcholine vesicles and the mechanism of graded release by amphipathic, α-helical peptides. *Biochemistry.* 43:8846–8857.
20. Kingsley, P. B., and G. W. Feigenson. 1979. The synthesis of a perdeuterated phospholipid: 1,2 dimyristoyl-*sn*-glycero-3-phosphocholine-d72. *Chem. Phys. Lipids.* 24:135–147.
21. Santoro, M. M., and D. W. Bolen. 1988. Unfolding free energy changes determined by the linear extrapolation method. 1. Unfolding of phenylmethanesulfonyl α-chymotrypsin using different denaturants. *Biochemistry.* 27:8063–8068.
22. Streicher, W. W., and G. I. Makhatadze. 2007. Unfolding thermodynamics of Trp-cage, a 20 residue miniprotein, studied by differential scanning calorimetry and circular dichroism spectroscopy. *Biochemistry.* 46:2876–2880.
23. De Levie, R. 1999. Estimating parameter precision in nonlinear least squares with Excel's Solver. *J. Chem. Educ.* 76:1594–1598.
24. Spolar, R. S., J. R. Livingstone, and M. T. Record, Jr. 1992. Use of liquid hydrocarbon and amide transfer data to estimate contributions to thermodynamic functions of protein folding from the removal of nonpolar and polar surface from water. *Biochemistry.* 31:3947–3955.
25. Murphy, J., K. Knutson, and A. Hinderliter. 2009. Protein-lipid interactions role of membrane plasticity and lipid specificity on peripheral protein interactions. *Methods Enzymol.* 466:431–453.
26. Kertz, J. A., P. F. Almeida, …, A. Hinderliter. 2007. The cooperative response of synaptotagmin I C2A. A hypothesis for a Ca^{2+}-driven molecular hammer. *Biophys. J.* 92:1409–1418.
27. Zhang, X., J. Rizo, and T. C. Südhof. 1998. Mechanism of phospholipid binding by the C2A-domain of synaptotagmin I. *Biochemistry.* 37:12395–12403.
28. Privalov, P. L., and N. N. Khechinashvili. 1974. A thermodynamic approach to the problem of stabilization of globular protein structure: a calorimetric study. *J. Mol. Biol.* 86:665–684.
29. Kumar, S., C. J. Tsai, and R. Nussinov. 2002. Maximal stabilities of reversible two-state proteins. *Biochemistry.* 41:5359–5374.
30. Pokorny, A., and P. F. F. Almeida. 2005. Permeabilization of raft-containing lipid vesicles by delta-lysin: a mechanism for cell sensitivity to cytotoxic peptides. *Biochemistry.* 44:9538–9544.
31. Wyman, J., and S. J. Gill. 1990. Functional Chemistry of Biological Macromolecules. University Science Books, Mill Valley, CA.
32. Sheets, E. D., D. Holowka, and B. Baird. 1999. Membrane organization in immunoglobulin E receptor signaling. *Curr. Opin. Chem. Biol.* 3: 95–99.
33. Uversky, V. N., C. J. Oldfield, and A. K. Dunker. 2008. Intrinsically disordered proteins in human diseases: introducing the D2 concept. *Annu Rev Biophys.* 37:215–246.
34. Fong, J. H., B. A. Shoemaker, …, A. R. Panchenko. 2009. Intrinsic disorder in protein interactions: insights from a comprehensive structural analysis. *PLOS Comput. Biol.* 5:e1000316.
35. Uversky, V. N. 2011. Multitude of binding modes attainable by intrinsically disordered proteins: a portrait gallery of disorder-based complexes. *Chem. Soc. Rev.* 40:1623–1634.
36. Hübner, W., H. H. Mantsch, …, H. Hauser. 1994. Conformation of phosphatidylserine in bilayers as studied by Fourier transform infrared spectroscopy. *Biochemistry.* 33:320–326.
37. Cevc, G., G. Watts, and D. Marsh. 1981. Titration of the phase transition of phosphatidylserine bilayer membranes. Effects of pH, surface electrostatics, ion binding, and head-group hydration. *Biochemistry.* 20:4955–4965.
38. Hinderliter, A. K., J. Huang, and G. W. Feigenson. 1994. Detection of phase separation in fluid phosphatidylserine/phosphatidylcholine mixtures. *Biophys. J.* 67:1906–1911.
39. Hinderliter, A., R. L. Biltonen, and P. F. Almeida. 2004. Lipid modulation of protein-induced membrane domains as a mechanism for controlling signal transduction. *Biochemistry.* 43:7102–7110.
40. Hinderliter, A., P. F. F. Almeida, …, R. L. Biltonen. 2001. Domain formation in a fluid mixed lipid bilayer modulated through binding of the C2 protein motif. *Biochemistry.* 40:4181–4191.
41. Rufener, E., A. A. Frazier, …, D. S. Cafiso. 2005. Membrane-bound orientation and position of the synaptotagmin C2B domain determined by site-directed spin labeling. *Biochemistry.* 44:18–28.

42. Frazier, A. A., C. R. Roller, …, D. S. Cafiso. 2003. Membrane-bound orientation and position of the synaptotagmin I C2A domain by site-directed spin labeling. *Biochemistry.* 42:96–105.

43. Zemel, A., A. Ben-Shaul, and S. May. 2004. Membrane perturbation induced by interfacially adsorbed peptides. *Biophys. J.* 86:3607–3619.

44. Zemel, A., A. Ben-Shaul, and S. May. 2008. Modulation of the spontaneous curvature and bending rigidity of lipid membranes by interfacially adsorbed amphipathic peptides. *J. Phys. Chem. B.* 112:6988–6996.

45. Zhang, Z., E. Hui, …, M. B. Jackson. 2010. Regulation of exocytosis and fusion pores by synaptotagmin-effector interactions. *Mol. Biol. Cell.* 21:2821–2831.

46. Takahashi, H., V. Shahin, …, J. M. Edwardson. 2010. Interaction of synaptotagmin with lipid bilayers, analyzed by single-molecule force spectroscopy. *Biophys. J.* 99:2550–2558.

47. Zucker, R. S., and W. G. Regehr. 2002. Short-term synaptic plasticity. *Annu. Rev. Physiol.* 64:355–405.